[6]Oosthuizen, P. H., "Profile Measurements in Vertical Axisymmetric Buoyant Air Jets," 6th International Heat Transfer Conf., Vol. 1, Toronto, Canada, 1978, pp. 103–108.

[7]Sherif, S. A., and Pletcher, R. H., "Measurements of the Thermal Characteristics of Heated Turbulent Jets in Cross Flow," *Journal of Heat Transfer*, Vol. 111, No. 4, 1989, pp. 897–903.

[8]Andreopoulos, J., "Heat Transfer Measurements in a Heated Jet-Pipe Flow Issuing into a Cold Cross Stream," *Physics of Fluids*, Vol. 26, No. 11, 1983, pp. 3201–3210.

[9]Andreopoulos, J., "On the Structure of Jets in a Crossflow," *Journal of Fluid Mechanics*, Vol. 157, 1985, pp. 163–197.

[10]Sherif, S. A., and Pletcher, R. H., "Measurements of the Flow and Turbulence Characteristics of Round Jets in Crossflow," *Journal of Fluids Engineering*, Vol. 111, No. 2, 1989, pp. 165–171.

[11]Andreopoulos, J., "Measurements in a Pipe Flow Issuing Perpendicularly into a Cross Stream," *Journal of Fluids Engineering*, Vol. 104, No. 4, 1982, pp. 493–499.

[12]Andreopoulos, J., and Rodi, W., "Experimental Investigation of Jets in a Crossflow," *Journal of Fluid Mechanics*, Vol. 138, 1984, pp. 93–127.

[13]Krausche, D., and Fearn, R. L., "Round Jet in a Cross Flow: Influence of Injection Angle on Vortex Properties," *AIAA Journal*, Vol. 16, No. 6, 1978, pp. 636, 637.

[14]Moody, F. J., and Amos, B. T., "A Procedure for Predicting Temperature Loadings for Thermal Stress Calculations in Thick-Walled Pipes," ASME Special Publication PVP-91, 1984, pp. 45, 46.

[15]Konduri, R., Khodabakhsh-Sharifabad, F., Idem, S., Munukutla, S., Bosi, D., Kirkendall, S., and Shrivastava, H., "Transient Thermal Mixing in the Feedwater Line of a Nuclear Power Plant," International Power Generation Conf., Paper 91-JPGC-Pwr-16, San Diego, CA, 1991.

Thermal and Hydrodynamic Behavior in Flow Networks

Wen-Jei Yang* and Nengli Zhang†
University of Michigan, Ann Arbor, Michigan 48109
and
S. Umeda‡
Fukuyama University, Fukuyama, Japan

Nomenclature

D = hydraulic diameter of ducts, cm
H_1, H_2 = water levels in upper tank and lower tank, respectively, cm
Nu = Nusselt number
q = heat flux, W/m^2
Re = Reynolds number
V = average velocity of the fluid in ducts, cm/s
V_i = local velocity of the fluid in ducts, cm/s
x = distance from inlet, cm
θ = intersection angle, deg

Subscripts
b = bottom and top
e = entrance
in = inner
L = left duct
o = outlet
out = out
R = right duct

Received Aug. 25, 1992; revision received Dec. 22, 1992; accepted for publication Dec. 22, 1992.

*Professor, Department of Mechanical Engineering and Applied Mechanics. Associate Fellow AIAA.
†Research Associate, Department of Mechanical Engineering and Applied Mechanics.
‡Professor, Department of Civil Engineering.

Introduction

A SYSTEM of mutually intersecting flow passages inside a plate or an assembly of plates, as shown in Fig. 1, is called a flow network. It has been discovered that a ramming of mutually intersecting flows results in a significant increase in convective heat transfer performance. Therefore, flow networks may serve as effective heat transfer devices with potential applications in industry, i.e., plate-type heat exchangers. Unfortunately, both theoretical and experimental investigations dealing with fluid flow and heat transfer in the networks are not available. Recently, a number of studies have been conducted to determine the pressure drop and heat transfer performance inside flow networks: Zhang et al.[1] conducted an experimental study on flow characteristics in flow networks with various geometries. In it, the intersecting pressure loss coefficient was defined and its magnitude determined as a function of geometric and flow conditions and a physical model was developed to predict the intersection pressure loss. The study concluded that a network with an intersection angle of 60 deg is the optimal geometry for the minimum intersecting pressure loss. Two additional investigations followed to aid in further understanding the flow behavior and heat transfer performance in the optimal flow network. The first used the hydrogen bubble method to observe flow patterns and mixing behavior in the intersection channel.[2] The second was a systematic measurement on the local heat transfer performance.[3] Both equal and unequal isoheat fluxes between the walls were treated. Recently, a hydraulic test setup of flow networks was constructed by Umeda et al.[4] for 1) a flow visualization study using both the dye injection and hydrogen bubble methods, 2) flow measurements by means of the laser Doppler velocimetry, and 3) pressure measurements using a piezometer.

This Note combines and compiles the results from the above-mentioned four investigations and explains in detail the mechanics of fluid flow and heat transfer in the flow networks.

Hydrodynamics in Flow Networks

Figure 1 is a schematic of a hydraulic recirculating flow system for testing flow inside two intersecting square ducts. The flow network was placed between two head tanks separated by a distance of 30 cm. The water level in the upper tank was maintained at a higher head of H_1 and that in the lower tank at a lower head of H_2. The difference $(H_1 - H_2)$ caused a flow through the two ducts with an intersection angle of q. A pump was employed to recirculate the flow. Each duct was square, 1.5 × 1.5 cm in cross section, and made of

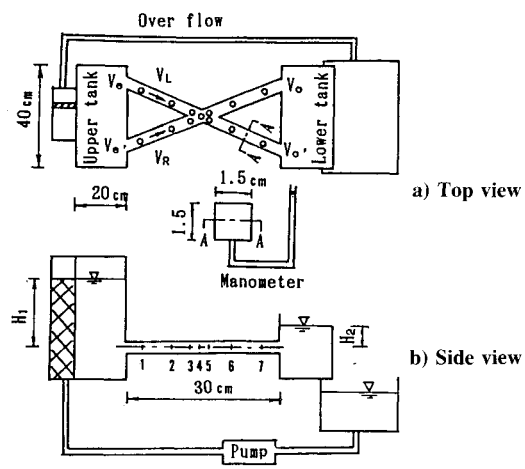

Fig. 1 Schematic of hydraulic recirculating flow system.

acrylic for illumination and observation. Three intersection angles were tested: 30, 60, and 90 deg. Both the flow rate and pressure in the network were varied by changing the magnitude of $H_1 - H_2$. Small holes were drilled at strategic locations on the bottom of the flow passages for pressure measurements using a manometer. The velocity was measured at various locations by means of a laser Doppler anemometry.

The hydrodynamic experiments were conducted under the conditions listed in Table 1, where q denotes the intersecting angle; H_1, H_2, heads of the upper and lower tanks, respectively; and V_L, V_R, average velocities of the left and right channels, respectively.

Figure 2 is a schematic of a representative photograph, for $q = 60$ deg and $V = 32.2$ cm/s, obtained from flow visualization using the dye injection method. The following observations are made in the figure: 1) formation of a flow divider, resulting from the collision of two streams of equal strength; 2) creation of a curved flow whose radius of curvature is related to $(p - q)$, inducing the centrifugal force and secondary flow effect; 3) formation of a flow separation zone at the corner downstream of the midplane; and 4) existence of four distinct flow regimes: the hydrodynamic entrance regime with the velocity on the inner wall side being lower than that on the outer wall side, the initial centrifugal region upstream of the intersection zone where the centrifugal force begins to take effect, the intersecting region with the flow divider, and the final centrifugal regime with higher velocity closer to the inner duct wall than the outer wall. The observation shown in Fig. 2 is supported by the pressure drop distribution in Fig. 3. The pressure drop continues in the entrance region, as in all straight tubes and ducts. It begins to recover at the second measurement location, suggesting the end of the entrance region and the beginning of the initial centrifugal regime. Then, a drastic change in the pressure drop curve characterizes the intersection zone, with a maximum followed by a minimum value. Thereafter comes the fourth flow regime in which the pressure head continues to recover (with a dent in a few rare occasions).

Figure 4 shows the results of velocity measurement in the flow network of $q = 60$ deg, using the laser Doppler velocimetry (LDV) method. It is seen that downstream of the

Table 1 Hydrodynamic experiment conditions

Run	θ	H_1, cm	H_2, cm	V_L, cm/s	V_R, cm/s
1	30 deg	2.7	2.1	22.5	22.5
2		4.6	3.2	33	32.6
3		11.9	2.2	97.1	96.3
4		14.1	2.1	105.6	109.9
5	60 deg	4.1	2.2	34.9	36.2
6		8.3	2.3	64	63.2
7		14.4	2.2	95.2	100.1
8		17.3	2.0	110	110.8
9	90 deg	5.4	2.0	49.3	48
10		8.4	2.0	73.5	69.4
11		14.3	2.0	95.3	95.4
12		18.2	2.0	104.7	107.4

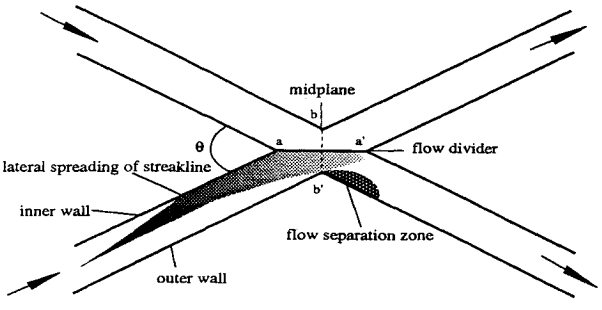

Fig. 2 Schematic of flow behavior revealed by the dye injection method.

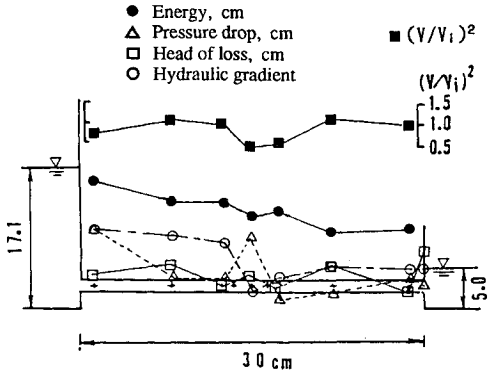

Fig. 3 Pressure drop distribution in the flow network with $q = 60$ deg.

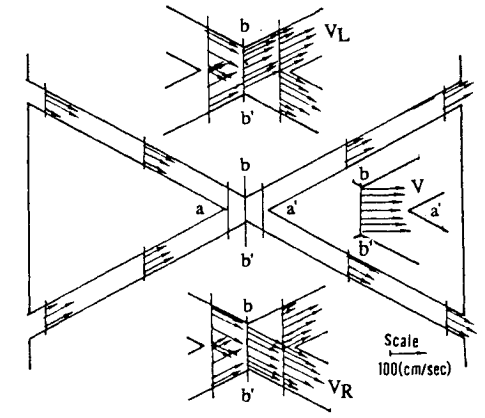

Fig. 4 Local velocities in the flow network with $q = 60$ deg.

inner wall intersection edge a, the two streams have identical velocity profiles crossing each other at an angle of q. The horizontal velocity distribution on the "midway" plane, $b - b'$, is symmetrical with respect to $a - a'$, having a small dent at the flow divider. V signifies the velocity at the midway plane which is the vector sum of its components V_L and V_R. The flow stream from the midway is practically uniform, while that downstream takes a substantial reduction in the velocity near the outer wall, evidence of a flow separation region. Figure 4 also indicates the switching of higher velocity on the outer wall side in the entrance region to the inner wall side in the final centrifugal regime.

Heat Transfer in Flow Networks

Figure 5 depicts the heat transfer experimental system which consists of an air filter, two rotometers covering the flow rate (2.03×10^{-3} to 1.22×10^{-2} m³/s), a plenum for stabilizing air flow, a glass thermometer, a high-accuracy pressure meter, a multipoint switchable thermometer, and a test section. Electrical power was supplied to four stainless-steel heating foils which were separately attached to the four channel walls. Two group isoheat-flux experiments were conducted to test the effect of unequal isoheat-flux of the walls on heat transfer performance in the flow network: the first, for equal heat flux between the side walls and the top-bottom walls and the second, for a case in which the heat flux of the side walls is four times greater than the heat flux of the top-bottom walls. In the present study, the Reynolds number ranges from 5000 to 30,000 (from 2800 to 15,000 in the fluid flow tests).

Figure 6 gives typical distributions of the local heat transfer performance in the network. The features of the four flow regimes are evidenced in the Nu distribution curve. It begins with the entrance (thermal) region with the magnitude of Nu diminishing with x/D at a steeper slope. The second flow (initial centrifugal) regime follows with a mild decline in Nu. The mechanics of heat transfer in the intersection (third flow)

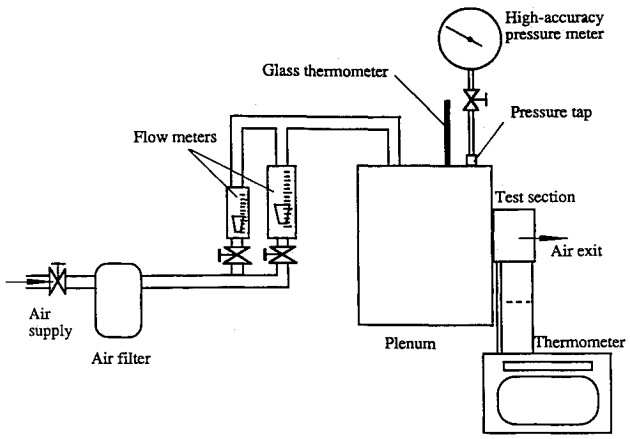

Fig. 5 Heat transfer experimental setup.

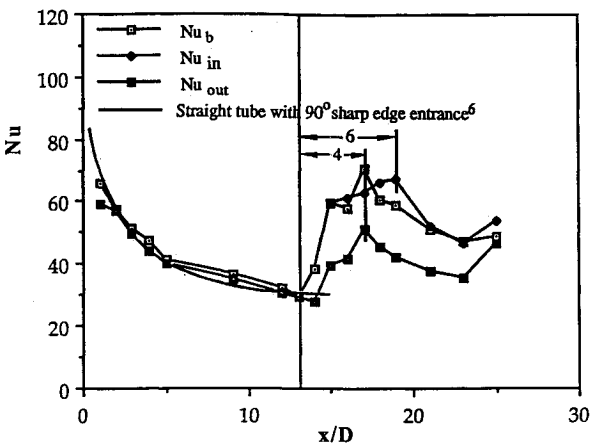

Fig. 6 Local Nusselt number for Re = 10,000; q = 1352.5 W/m^2.

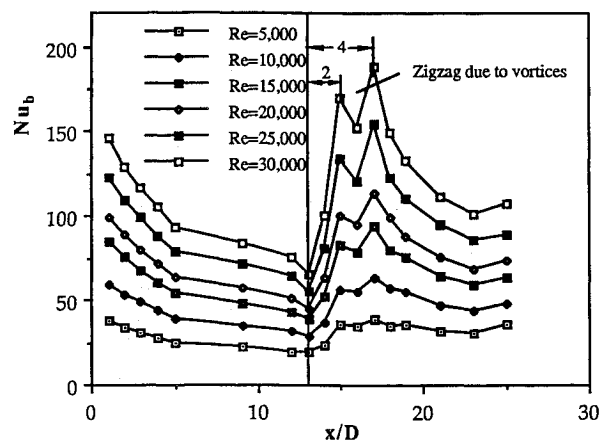

Fig. 7 Fluctuation of Nusselt number in the flow network.

region takes a different course depending upon the walls: the bottom (and top) and inner walls are characterized by a recovery in Nu beginning at the midway plane, but Nu of the outerwall continues to slide with x/D. In the fourth flow (final centrifugal) regime, all four walls undergo a significant heat transfer enhancement immediately after the intersection zone, reaching a maximum, followed by a decline toward the duct exit. However, one special event is seen to occur near the duct exit. This appearance of the thermal exit effect brings the number of thermal flow regimes in the flow network to five. Note that the monotonically decreasing line represents the Nu performance in a straight tube with 90-deg sharp-edge entrance. It is superposed in the figure for comparison. One additional feature in the fourth thermal flow regime is a zigzag in the Nu vs x/D curves around two to four times d downstream of the midway plane (i.e., flow intersection center) as seen in Fig. 7. The fluctuation of the Nusselt number of the bottom wall (Nu_b) is enhanced by increasing the Reynolds number. It can be explained by the action of vortices existing in this region. The same effects of the Reynolds number on the local Nusselt number also occurred on the inner and outer walls (not shown). However, the zigzag in Nu_{in} vs x/D curves is not so evident, and the heat transfer augmentation is caused by the flow impact on the right wall.

Conclusions

Thermal and hydrodynamic behavior in flow networks have been brought to light. Discussion is based upon equal flow rates in both ducts and the intersection angle of 60 deg which provides the optimal intersection pressure loss. It is disclosed that the formation of a flow divider in the intersection zone results in each stream following a curved flow path, shifting from the left to the right ducts and vice versa. The effect of a centrifugal force is therefore brought into play in the flow network. Four hydrodynamic flow regimes are identified through flow visualization, LDV and pressure measurements. The mechanisms of heat transfer in each of these four flow regimes are uniquely different, with an additional feature of thermal exit effect near the duct outlet.

References

[1]Zhang, N., Yang, W.-J., Xu, Y., and Lee, C. P., "Flow Characteristics in Flow Networks," *Experiments in Fluids*, Vol. 14, 1993, pp. 25–32.

[2]Zhang, N., Yang, W.-J., Xu, Y., and Lee, C. P., "An Application of Hydrogen Bubble Method to Flow Networks," *Flow Visualization VI*, edited by Y. Tanida and H. Miyashiro, Springer-Verlag, Berlin, 1992, pp. 90–96.

[3]Zhang, N., Yang, W.-J., and Lee, C. P., "Local Heat Transfer in Flow Networks," *Transport Phenomena Science and Technology*, Higher Education Press, Beijing, China, 1992, pp. 296–301.

[4]Umeda, S., and Yang, W.-J., "Mechanics and Correlations of Flow Phenomena in Intersecting Ducts," *Experiments in Fluids* (submitted for publication).

[5]Bunditkul, S., and Yang, W.-J., "Laminar Transport Phenomena in Parallel Channels with a Short Flow Construction," *Journal of Heat Transfer*, Vol. 101, No. 2, 1979, pp. 217–223.

[6]Mills, A. F., "Experimental Investigation of Turbulent Heat Transfer in the Entrance Region of a Circular Conduct," *Journal Mechanical Engineering Science*, Vol. 4, No. 1, 1962, pp. 63–77.

AlCl Absorption Feature in Solid Rocket Plume Radiation

W. K. McGregor,* J. A. Drakes,† K. S. Beale,‡ and F. G. Sherrell‡
Sverdrup Technology, Inc.,
Arnold Air Force Base, Tennessee 37389

Introduction

WHEN a high resolution ultraviolet scanning monochromator is pointed normal to the axis of an exhaust plume

Presented as Paper 92-2917 at the AIAA 27th Thermophysics Conference, Nashville, TN, July 6–8, 1992; received Aug. 7, 1992; revision received Dec. 10, 1992; accepted for publication Dec. 15, 1992.

*Senior Technical Specialist, AEDC Group, Arnold Engineering Development Center. Associate Fellow AIAA.

†Physicist, AEDC Group, Arnold Engineering Development Center. Senior Member AIAA.

‡Engineer, AEDC Group, Arnold Engineering Development Center.